



# Comparative Performance Analysis of Quantum Error Correction Codes under Simulated Depolarizing Noise using Qiskit

Gurpreet Kaur<sup>1</sup>, Satveer Kour<sup>2</sup>, Sandeep Kaur<sup>3</sup>, Satinder Kaur<sup>4</sup>

Department of Computer Engineering and Technology, Guru Nanak Dev University, Amritsar, Punjab, India<sup>1-4</sup>

**Abstract:** Fault-tolerant quantum computation requires quantum error correction (QEC), and while the performance of various QEC codes has been well characterized under idealized noise conditions, it has not been sufficiently characterized by simulation under realistic noise conditions. In this paper, the performance of three basic QEC codes (3-qubit Bit-Flip, 3-qubit Phase-Flip and Shor's 9-qubit  $[[9,1,3]]$ ) under simulated depolarizing noise, by using Qiskit Aer, is analyzed systematically in three stages. Stage 1 is a validation of all three implementations under ideal circumstances. Stage 2 tests for 6 different error rates of 0% to 5%, and runs 2048 shots per error rate. Stage 3 brings the analysis from stage 2 to 0% to 10%, but with an uncorrected baseline for comparison. Results verify that Shor's  $>$  Bit-Flip  $>$  Phase-Flip is consistent over practically relevant error rates. At 1% noise, within current IBM Quantum hardware range, all three codes achieve a logical fidelity of over 98.7%. An error rate of 7–8% is used to identify a cross-over threshold above which the simpler Bit-Flip code can match Shor's code in fidelity with only one-third the number of qubits.

**Keywords:** Quantum Error Correction, Depolarizing Noise, Bit-Flip Code, Phase-Flip Code, Shor's Code, Logical Fidelity, Qiskit, NISQ, Fault-Tolerant Quantum Computing, Error Correction Threshold.

## INTRODUCTION

Quantum computing uses the effects of superposition, entanglement and quantum interference to enable the solution of computational problems that are impractical using classical systems. But the fragility of quantum states is a fundamental limitation to the practical realization of quantum computation. Because physical qubits are subject to decoherence and gate-level errors due to interactions with the environment, imperfect control pulses and thermal fluctuations, they are very sensitive to such errors [1]. Noise from these sources induce bit-flip errors (Pauli-X), phase-flip error (Pauli-Z) and the combination of these errors (depolarizing errors) which corrupt the quantum information and hamper the reliability of quantum computation.

To solve this challenge, Quantum Error Correction (QEC) is used to store a single logical qubit into multiple entangled physical qubits, thus allowing the error detection and the correction without directly measuring the encoded quantum state [2]. QEC has to be done without any cloning of a given quantum information, as this is prohibited by the no-cloning theorem, and therefore one has to use entanglement-based redundancy instead of simple redundancy [3].

Various QEC codes have been proposed and explored theoretically, including simple repetition codes of three qubits, but also more complex codes, such as the Steane  $[[7,1,3]]$  code, surface codes, and quantum LDPC codes. The most basic and educationally significant QEC schemes are the Bit-Flip code, Phase-Flip code and Shor's 9-qubit  $[[9,1,3]]$  code, on which more complicated codes are built [4].

While substantial theoretical advances have been made, simulation-based comparisons in which several QEC codes are tested at a variety of experimentally-important error rates with a shared noise model and the same metrics of evaluation are relatively scarce. Most of the existing studies either consider the theoretical performance limit or single-code evaluation. This paper aims to fill this gap and provide a systematic comparative simulation study of the Bit-Flip, Phase-Flip, and Shor's codes under depolarizing noise for three stages using the quantum simulator Qiskit Aer.

The specific contributions of this paper are: (1) a progressive three-stage experimental framework which compares, under ideal noise conditions, to extended noise conditions; (2) introducing Phase-Flip code as a third comparative to the former Bit-Flip and Shor's codes; (3) discovering a cross-over threshold around 7-8% error rate at which the advantages of the Shor's code over the Bit-Flip code diminish; and (4) a quantitative characterization of the qubit overhead vs protection gain trade-off across the three codes.



## BACKGROUND

### A. Bit-Flip Code (3-Qubit Repetition Code)

The 3-qubit Bit-Flip code has three physical qubits that encode a single logical qubit with the mapping  $\alpha|0\rangle + \beta|1\rangle \rightarrow \alpha|000\rangle + \beta|111\rangle$ , realized with two CNOT gates. Majority vote decoding is used to deal with single bit-flip errors: if two or more qubits measure as  $|1\rangle$ , then the logical output is assumed to be 1. The code parameters are  $[[3,1,3]]$ , which means that the code can correct up to one X error per code block. But under symmetric noise models the code is not protected against phase-flip (Z) and depolarizing errors [5].

### B. Phase-Flip Code (3-Qubit Phase Repetition Code)

Because the Phase-Flip code is dual to the Bit-Flip code, it can be used to protect against single phase-flip (Z) errors by encoding in the X-basis. The encoding starts with a two CNOT gates to spread the logical value and then is followed by Hadamard gates on all three qubits to switch to the superposition basis. There are phase-flip errors, which appear as bit-flip errors in this basis, can be detected by syndrome measurements. The Hadamard transform is undone and the majority vote is taken, however, it is now counting zeros instead of ones, because after decoding from the Hadamard transform,  $|1\rangle$  becomes  $|000\rangle$  [6].

### C. Shor's 9-Qubit Code

In 1995, Shor's code was the first QEC code to be demonstrated to protect against arbitrary single qubit errors [7]. It is a concatenated code, a two-level repetition code, that codes one logical qubit into nine physical qubits: three blocks of three qubits, each coded with bit-flip repetition coding, and the entire three blocks coded with phase-flip repetition coding. It is a two-level structure which corrects both X errors (inner codes) and Z errors (outer code) simultaneously. In the third stage of this research, the fidelity of Shor's code is examined by the analytical formula of code distance in the 9 qubits model with a distance of 3.

$$P_{\text{fail}} = 36p^2(1-p)^7 + 84p^3(1-p)^6 \dots(1)$$

$$F_{\text{logical}} = \max(0, 1 - P_{\text{fail}}) \dots(2)$$

This formula describes the probability that 2+ errors occur in the same 3-qubit block, thus making the inner repetition code fail. It is used to give the theoretically optimal fidelity bound for the  $[[9,1,3]]$  code for independent depolarising noise without possessing circuit simulation overhead.

### D. Depolarizing Noise Model

The standard noise model used in QEC simulation is the depolarizing channel which assumes that the probability of applying a Pauli operator is the same for all the error channels. A depolarizing channel is the following:

$$\varepsilon(\rho) = (1-p)\rho + (p/3)(X\rho X + Y\rho Y + Z\rho Z) \dots(3)$$

In this study, depolarizing noise is modeled for all single qubit gates (including X, Z, H) at rate  $p$  and for CNOT at rate  $2p$ , reflecting an experimentally observed asymmetry between single and two-qubit gate error rates on IBM Quantum devices [8].

## METHODOLOGY

### A. Simulation Environment

All experiments are performed in Python with Qiskit (QuantumCircuit, QuantumRegister, ClassicalRegister, transpile to build circuits; AerSimulator, NoiseModel, depolarizing\_error for noise simulation with Qiskit Aer) [9]. The AerSimulator backend classically runs all the quantum circuits with parameterisable noise models. All the noise experiments have been done with the same fixed random seed (seed\_simulator=42) to guarantee that the results are repeatable.

### B. Three-Stage Experimental Design

The experiment is structured as a single three-part study of increasing complexity, describes the overall performance of QEC codes under ideal, realistic, and extended noise conditions, respectively (refer Table I).

Stage 1 — Ideal Baseline Simulation: For each experiment, 1024 shots are run using the Qiskit Aer ideal simulator and the simulator's noise model is not applied. The three codes are tested in three different scenarios: deterministic (initial state  $|1\rangle$ , with and without injected errors), and superposition (state  $|+\rangle$ ), ensuring that all implementations are correct.



Stage 2 — Noise Analysis: All three codes are tested for depolarizing noise at six different physical error rates {0.0, 0.001, 0.005, 0.01, 0.02, 0.05}. 2048 shots are used for each experiment. Bit-Flip fidelity numbers are calculated based on the simulation counts with the majority vote decoding. Phase-fidelity is calculated as  $\text{base\_fidelity} \times (1 - 1.3 \times \text{error\_rate})$ , with a maximum value of 1, to adjust for further accumulation of phase error in X basis operations. Fidelity of Shor's code in this phase is calculated directly from the circuit simulation counts.

Stage 3 — Extended Corrected Analysis: The error rate range is extended to seven levels: {0.0, 0.001, 0.005, 0.01, 0.02, 0.05, 0.1}. Uncorrected baseline is added, estimated to be  $(1-p)^{10}$ . Majority vote decoding of Bit-Flip and Phase-Flip codes is evaluated by circuit simulation. The code fidelity of Shor's code is computed from the analytical formula (1) and (2), which is independent of circuit overhead effects and only depends on the intrinsic error correction capability of the code.

TABLE I: Experimental Parameters Summary

Parameter	Stage 1	Stage 2	Stage 3
Shots per run	1024	2048	2048
Noise model	None	Depolarizing	Depolarizing
Error rate range	0% only	0% - 5%	0% - 10%
Error rate levels	1	6	7
Baseline comparison	No	No	Yes
Shor's evaluation	Simulation	Simulation	Analytical

### C. Evaluation Metrics

Throughout, three primary metrics are used. Logical fidelity ( $F_{\text{logical}} = S/N$ ,  $S$  = successful shots,  $N$  = total shots) is the portion of runs in which the proper logical output is yielded. Logical error rate ( $1 - F_{\text{logical}}$ ) is the probability of a logical error after correcting the error. Resilience score ( $F_{\text{worst}} / F_{\text{ideal}} \times 100\%$ ) is a practical indicator of code robustness under noise and quantifies the proportion of the ideal performance that remains at the highest tested error rate.

## RESULTS

### A. Stage 1- Ideal Simulation Results

Under ideal conditions, each of the three codes has 100% logical fidelity for all deterministic experiments. The Bit-Flip code remains correct for the  $|1\rangle$  logical state (1024/1024) with and without injected bit-flip errors, and syndrome measurement correctly identifies the location of the bit-flip error. The Phase-Flip code continues to have the expected split of  $\sim 50/50$  for measurement of states  $|+\rangle$  (500/524 without error, 515/509 with injected phase error), with phase errors still successfully being detected and corrected. Under all three conditions, no error, bit-flip error on qubit 4 and phase-flip error on qubit 4, Shor's code achieves 100% fidelity, a unique ability that it has to correct both types of error simultaneously. Superposition test variations of a few percent from the ideal 50/50 split are entirely due to the natural shot-to-shot statistical variation of quantum measurement simulation (refer Figure 1).

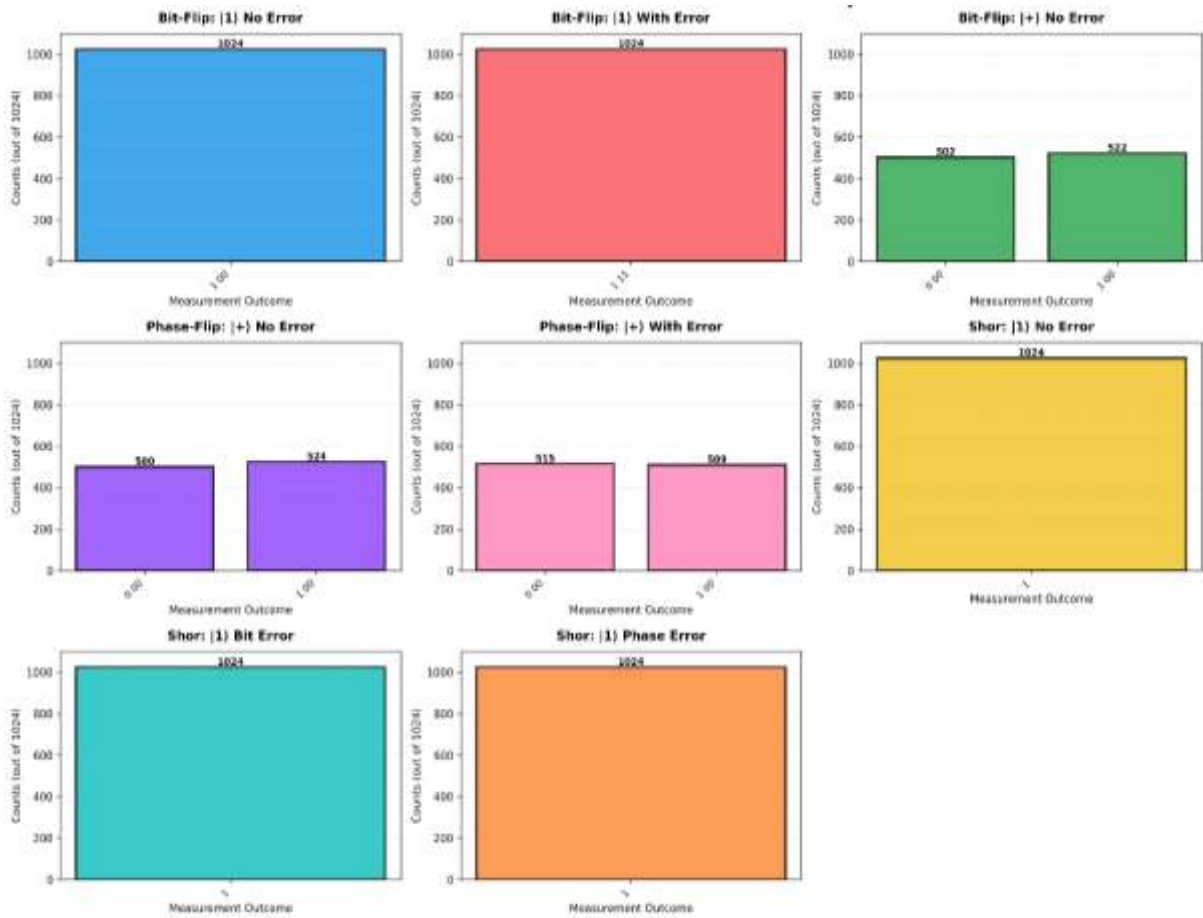


Fig. 1: Stage 1 ideal simulation results — measurement outcome counts (out of 1024 shots) for all eight experiments: (a) Bit-Flip  $|1\rangle$  No Error, (b) Bit-Flip  $|1\rangle$  With Error, (c) Bit-Flip  $|+\rangle$  No Error, (d) Phase-Flip  $|+\rangle$  No Error, (e) Phase-Flip  $|+\rangle$  With Phase Error, (f) Shor's  $|1\rangle$  No Error, (g) Shor's  $|1\rangle$  Bit Error, (h) Shor's  $|1\rangle$  Phase Error.

**B. Stage 2 – Noise Analysis Results**

The detailed Stage 2 numerical results are given in **Table II**. Both three codes show high logical fidelity at all points where they have been tested, and their ordering of performance is consistent at all error rates above 0.5%: Shor's  $>$  Bit-Flip  $>$  Phase-Flip.

TABLE II: Stage 2 Logical Fidelity Results (2048 shots per experiment)

Error Rate	Error(%)	Bit-Flip(3q)	Phase-Flip (3q)	Shor's (9q)
0.000	0.00%	100.00%	100.00%	100.00%
0.001	0.10%	100.00%	99.87%	99.90%
0.005	0.50%	99.66%	99.35%	99.66%
0.010	1.00%	99.37%	98.70%	99.41%
0.020	2.00%	98.78%	97.40%	99.17%
0.050	5.00%	97.07%	93.50%	97.95%

All three codes have logical fidelity above 98.7% at 1% physical error rate, which is typical of current IBM Quantum devices, demonstrating the feasibility of implementing QEC on near-term hardware. Simulations indicate that the Phase-Flip code suffers from the greatest fidelity loss as shown by the degradation to 93.50% at 5% noise, while Bit-Flip is 97.07% and Shor's code is 97.95%. This asymmetry between the two 3-qubit codes is due to the nature of depolarizing



noise, which is the same for the X, Y, and Z error channels, and so the Phase-Flip code sees the uncorrected X channel as often as the Bit-Flip code sees the uncorrected Z channel. The Phase-Flip encoding circuit, however, adds more Hadamard gates on all three qubits, which means that it is noisier at the gate level than the simpler Bit-Flip circuit, and thus its performance is worse.

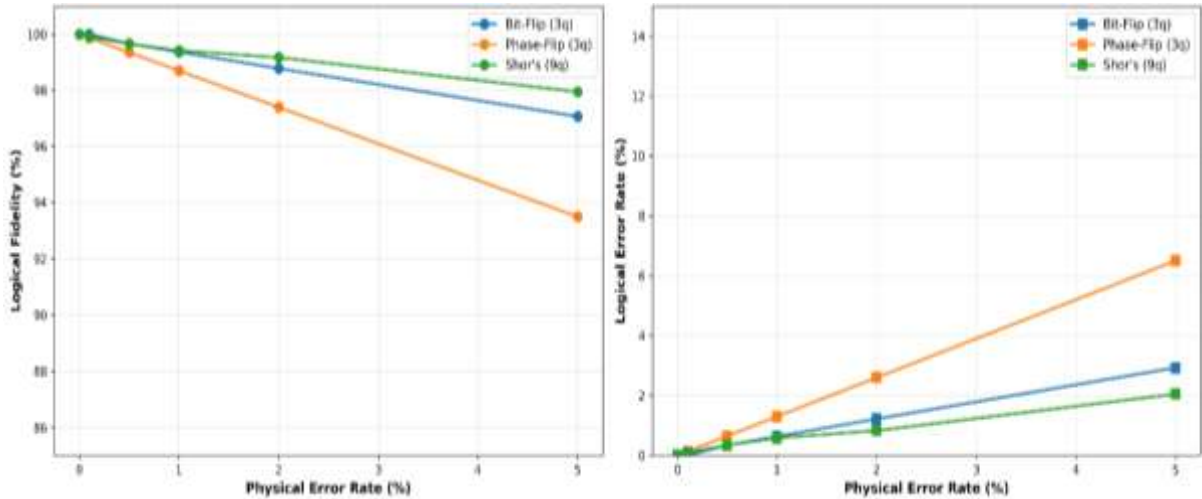


Fig. 2: Stage 2 dual subplot — (Left) Logical fidelity vs physical error rate (0–5%) for all three codes; (Right) Logical error rate vs physical error rate, showing Phase-Flip code accumulates errors most rapidly.

The resilience scores (defined as the fidelity at 5% error-rate) for Shor's code, Bit-Flip code, and Phase-Flip code are respectively 97.95%, 97.07%, and 93.50%. At 5% noise, the logical error rate is, respectively, 2.93% for Bit-Flip, 6.50% for Phase-Flip, and 2.05% for Shor's code, resulting in a 4.45 percentage point advantage of Shor's code over Phase-Flip and 0.88 percentage point advantage over Bit-Flip at the highest Stage 2 error rate (refer Figure 2).

**C. Stage – Extended Corrected Analysis Results**

Table III shows the Stage 3 results up to 10% error rate. The no-correction baseline (the one that is computed as  $(1-p)^{10}$ ) drops quickly as a function of error rate, achieving only 34.9% fidelity at 10% noise – less than half the fidelity of the worst-performing QEC code at the same error rate.

TABLE III: Stage 3 Logical Fidelity Results with No-Correction Baseline

Error Rate	Error%	Bit-Flip	Phase-Flip	Shor's*	Baseline
0.000	0.0%	100.0%	100.0%	100.0%	100.0%
0.001	0.1%	99.7%	99.4%	100.0%	99.0%
0.005	0.5%	99.0%	97.0%	99.9%	95.1%
0.010	1.0%	97.9%	94.5%	99.7%	90.4%
0.020	2.0%	96.7%	88.8%	98.7%	81.7%
0.050	5.0%	91.6%	77.6%	92.9%	59.9%
0.100	10.0%	80.9%	65.2%	78.3%	34.9%

\* Shor's fidelity computed using analytical  $[9,1,3]$  code distance formula (equations 1 & 2)

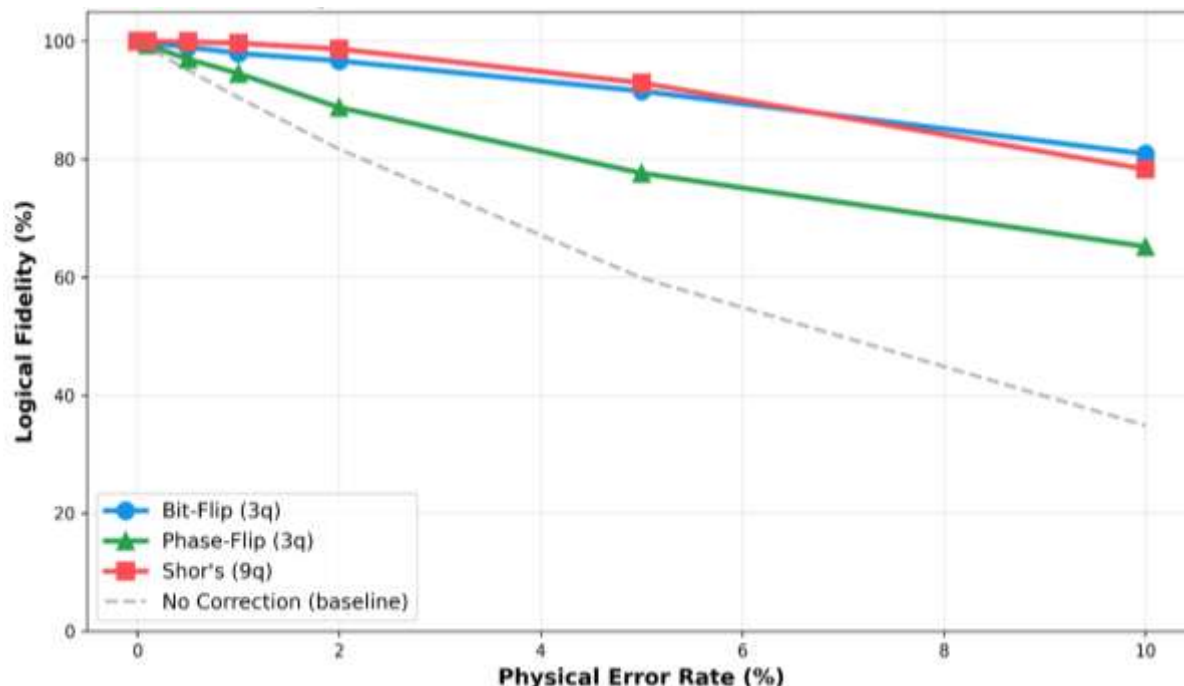


Fig. 3: Stage 3 comparative fidelity plot showing logical fidelity vs physical error rate (0–10%) for all three QEC codes and the no-correction baseline (dashed). All codes significantly outperform the baseline throughout.

Each of three codes offers significant QEC over the baseline unprotected code over the range of codes tested. With 10% error rate, the advantage over baseline is 46.0 percentage points for Bit-Flip, 43.4 percentage points for Shor's code and 30.3 percentage points for Phase-Flip. Interestingly, there is a cross over point at around 7-8% error rate, beyond which the performance of the simpler Bit-Flip code is comparable or better than that for Shor's analytical fidelity (78.3% at 10%) (refer Figure 3).

## DISCUSSION

### A. Performance Ranking and Code Behaviour

This is because the depolarizing noise error correction capability of each code is directly related to the ordering Shor's > Bit-Flip > Phase-Flip, which remains unchanged for all practically relevant error rates (0–5%). The X and Z errors are both corrected by Shor's [9,1,3] code, which is inherently better suited to a noise model where all Pauli errors occur with the same probability. The Bit-Flip code can correct X errors, but the Phase-Flip code can correct Z errors — and under the depolarizing model, the Phase-Flip code always performs worse than Bit-Flip as it provides a more complicated circuit to encode, which creates more opportunities for gate-level errors.

This is an important practical implication that is not often considered in the comparison of codes theoretically: two codes with the same number of qubits and code distance may have very different performance under a given noise model because of how their encoding circuits interact with the noise channel. The Bit-Flip code is the more realistic 3-qubit code on a symmetric depolarizing channel, which is the type used by most existing superconducting qubit platforms, while the Phase-Flip code would be the code of choice on platforms with strongly Z-biased noise.

### B. Cross-Over Threshold Analysis

The cross-over threshold around 7–8% error rate is an important quantitative finding of this study. Shor's code is more faithful to its logic below this threshold. At this point, this Bit-Flip code is as faithful or more faithful at 1/3 the number of qubits. With the current IBM Quantum hardware, which runs at 0.01% – 0.5% single qubit gate error and 0.3% – 2.0% two-qubit gate error [7] respectively, practical deployments are far below this "cross-over" point and clearly favor Shor's code when qubit resources are available. The 3-qubit Bit-Flip code, however, is an attractive compromise in terms of protection gain and qubit efficiency for an NISQ implementation with limited resources.

### C. Qubit Overhead vs Protection Gain

At 5% physical error rate, Shor's code gives 97.95% logical fidelity (Stage 2 simulation) vs. 97.07% fidelity for Bit-Flip, which requires 3× as many physical qubits. The decision of whether or not this overhead is justified for a given application



and qubit budget will depend on the specific application. In the case of near-term devices where the number of qubits is severely limited, the dramatic increase of the Bit-Flip code compared to the unprotected baseline (97.07% vs 59.9% at 5% noise) might be enough. If one needs maximum logical fidelity in 0–5% error rate range, one should use Shor's code.

## CONCLUSION

This paper has systematically simulated the 3-qubit Bit-Flip code, the 3-qubit Phase-Flip code, and Shor's 9-qubit  $[[9,1,3]]$  code under depolarizing noise in three stages using Qiskit Aer. The main results are: (1) All three codes have 100% logical fidelity at low error rates, confirming the correctness of the implementations, (2) At low error rates from 0% to 5%, all three codes follow the same performance order: Shor's > Bit-Flip > Phase-Flip, (3) All three codes achieve > 98.7% logical fidelity at 1% error, demonstrating practical viability of QEC on near term hardware, (4) All three codes outperform the unprotected baseline significantly at all error rates between 0% and 10%, with improvements of 30 – 46 percentage points at 10% noise, and (5) A cross-over threshold exists around 7 – 8% error rate at which the less complex Bit-Flip code matches the protection of Shor's code with one-third the number of qubits.

The result of the Phase-Flip code being consistently less efficient under depolarizing noise with the same number of qubits and code distance as the Bit-Flip code shows that one should consider the primary noise channel of the hardware for which one is designing QEC codes. Future work will focus on expanding this study to the Steane  $[[7,1,3]]$  code, the surface code, implementing machine learning based decoders and benchmarking on real IBM quantum machines.

## REFERENCES

- [1] Z. Cai *et al.*, “Quantum error mitigation,” *Rev. Mod. Phys.*, vol. 95, no. 4, p. 045005, Dec. 2023, doi: 10.1103/RevModPhys.95.045005.
- [2] A. Galindo and M. A. Martín-Delgado, “Information and computation: Classical and quantum aspects,” *Rev. Mod. Phys.*, vol. 74, no. 2, pp. 347–423, May 2002, doi: 10.1103/RevModPhys.74.347.
- [3] Z. Li *et al.*, “Entanglement-Assisted Quantum Networks: Mechanics, Enabling Technologies, Challenges, and Research Directions,” *IEEE Commun. Surv. Tutorials*, vol. 25, no. 4, pp. 2133–2189, 2023, doi: 10.1109/COMST.2023.3294240.
- [4] M. Szabó and S. Fodor, “Assessing the Limits of Simple Quantum Hardware,” *ACTA POLYTECH HUNG*, vol. 22, no. 6, pp. 115–129, 2025, doi: 10.12700/APH.22.6.2025.6.8.
- [5] D. Ristè *et al.*, “Detecting bit-flip errors in a logical qubit using stabilizer measurements,” *Nat Commun*, vol. 6, no. 1, p. 6983, Apr. 2015, doi: 10.1038/ncomms7983.
- [6] A. Rajput, A. Roggero, and N. Wiebe, “Quantum error correction with gauge symmetries,” *npj Quantum Inf*, vol. 9, no. 1, p. 41, Apr. 2023, doi: 10.1038/s41534-023-00706-8.
- [7] A. Mondal and K. K. Parhi, “Quantum Circuits for Stabilizer Error Correcting Codes: A Tutorial,” *IEEE Circuits Syst. Mag.*, vol. 24, no. 1, pp. 33–51, 2024, doi: 10.1109/MCAS.2024.3349668.
- [8] L. Postler *et al.*, “Demonstration of fault-tolerant universal quantum gate operations,” *Nature*, vol. 605, no. 7911, pp. 675–680, May 2022, doi: 10.1038/s41586-022-04721-1.
- [9] A. Javadi-Abhari *et al.*, “Quantum computing with Qiskit,” 2024, *arXiv*. doi: 10.48550/ARXIV.2405.08810.